RSC Advances

PAPER

View Article Online
View Journal | View Issue

Cite this: *RSC Adv.*, 2020, **10**, 32938

Lutetium-containing sinoporphyrin sodium: a water-soluble photosensitizer with balanced fluorescence and phosphorescence for ratiometric oxygen sensing†

Lixin Zang *[a] and Huimin Zhao*[b]

Development of a photosensitizer for ratiometric O_2 sensing is desirable for the precise treatment of cancer by photodynamic therapy. Herein, lutetium(III)-containing sinoporphyrin sodium (Lu-DVDMS) was designed as a phosphorescent photosensitizer to balance phosphorescence and fluorescence emissions for ratiometric O_2 sensing. Lu-DVDMS exhibited high water solubility, chemical stability, photostability, photosensitivity, and singlet-oxygen quantum yield of 0.23 ± 0.06. The phosphorescence and fluorescence quantum yields of Lu-DVDMS were 0.33 and 0.32%, respectively. Compared with the phosphorescence-to-fluorescence ratio (*R*) of gadolinium-DVDMS (Gd-DVDMS), which was >10, that of Lu-DVDMS was ~1, facilitating ratiometric O_2 sensing. The relatively weak phosphorescence-inducing effect of Lu(III) owing to the absence of paramagnetism, as compared to Gd(III), balanced the phosphorescence and fluorescence emissions of Lu-DVDMS. The fluctuation of *R* for Lu-DVDMS was approximately one-sixth of Gd-DVDMS, owing to the high signal-to-noise ratio simultaneously achieved for both phosphorescence and fluorescence emissions. The intensity and lifetime Stern–Volmer plots for Lu-DVDMS were 0.9840 + 0.0024[O_2] and 0.9517 + 0.0034[O_2], respectively ([O_2]: oxygen concentration). Fast response and recovery times (<2 min) were achieved. The precision of oxygen detection using Lu-DVDMS was better than 0.5 μM in the 0–400 μM oxygen detection range. Therefore, Lu-DVDMS is a potential phosphorescent photosensitizer for ratiometric O_2 sensing.

Received 20th June 2020
Accepted 25th August 2020

DOI: 10.1039/d0ra05400c

rsc.li/rsc-advances

Introduction

Photodynamic therapy (PDT) is the most advanced treatment method for many kinds of cancers.[1–3] PDT relies on the activation of a photosensitizer with light to generate highly cytotoxic reactive oxygen species, which kill the tumor cells.[4] PDT offers several advantages over traditional chemotherapies, including selective targeting and fewer side effects. However, the widespread clinical application of PDT has been hindered because its effects are not uniform among patients and PDT cannot yet be tailored to individual needs. To realize the precise treatment of cancer in individual patients by PDT, three elements must be controlled and managed quantitatively: the photosensitizer concentration, molecular O_2 concentration, and the light dose.[5,6] In particular, the distribution of O_2 in treated tissues can greatly affect the efficiency of PDT.[7] PDT efficiency is low when the local O_2 concentration in the tissue is inadequate,[8] even when the photosensitizer concentration in the tissue and light dosage are sufficient. Hence, the accurate measurement of O_2 during PDT is critical for successful treatment.

Most of the data on the O_2 concentration in tissue are collected using polarographic microelectrodes.[9,10] However, these microelectrodes are invasive, consume oxygen, and their usage is restricted to specific locations. Biological O_2-sensing techniques based on the quenching of room-temperature phosphorescence (RTP) of Pt- and Pd-porphyrins, pioneered by Wilson *et al.*,[11] have created new opportunities in the measurement of the O_2 concentration in tissues. Relatively strong RTP emissions have also been observed from Gd(III) porphyrins owing to significant mixing between its singlet and triplet states caused by the heavy atom effect (HAE), and strong paramagnetism and special energy levels of Gd(III).[5] RTP-based

[a]*College of Chemistry, Chemical Engineering and Materials Science, Collaborative Innovation Center of Functionalized Probes for Chemical Imaging in Universities of Shandong, Key Laboratory of Molecular and Nano Probes, Ministry of Education, Shandong Provincial Key Laboratory of Clean Production of Fine Chemicals, Shandong Normal University, Ji'nan 250014, China. E-mail: zanglixinxinyuan@163.com*

[b]*Shandong Provincial Engineering and Technical Center of Light Manipulations, Shandong Provincial Key Laboratory of Optics and Photonic Device, School of Physics and Electronics, Shandong Normal University, Ji'nan 250014, China. E-mail: hmzhao_hit@hotmail.com*

† Electronic supplementary information (ESI) available: Methods of measuring phosphorescence lifetimes; the purity of Lu-DVDMS; water solubility of DVDMS and HMME; singlet-oxygen quantum yield of Lu-DVDMS; quantum yield of Lu-DVDMS phosphorescence; stability and photostability of the O_2 indicator; response time for the O_2 indicator. See DOI: 10.1039/d0ra05400c

methods can overcome some limitations of polarography. They can be used to obtain images of O_2 distribution in tissues without being invasive or disturbing the local tissue environment.[5] Ratiometric approaches based on the ratio of the phosphorescence (O_2-dependent) to fluorescence (O_2-independent) emissions[12,13] can increase the sensing stability of a sensor by decreasing the non-analyte-induced intensity changes, such as fluctuations in the excitation light and photodetector, or the photobleaching of indicators.[14] Most importantly, there is no need for repetitive calibration of oxygen concentration in the ratiometric method.[14,15] A single indicator with dual emission can be a better O_2 indicator than a system with two luminophores (indicator and reference).[16,17] Comparable phosphorescence and fluorescence intensities from a single molecule are required to achieve high signal-to-noise ratios (SNRs) in ratiometric O_2 sensing.[18] However, Pt-, Pd-, and Gd-porphyrins are unsuitable as dual-emissive O_2 indicators because their fluorescence emissions are too weak to be used as reference signals.[19–22] Thus, it is desirable to develop suitable dual-emissive metalloporphyrins with comparable emissions for ratiometric O_2 sensing based on a single indicator.

To balance the RTP and fluorescence emissions, the energy allocation between the singlet and triplet excited states of the porphyrin derivative must be equalized. Lutetium(III) is a lanthanide ion that can show the HAE and the 4f sub-shell of lutetium(III) is filled. Lutetium(III) has no 4f energy levels; thus, the energy transfer from the porphyrin ligand to lutetium(III) is also impossible,[23] similar to the case of Gd(III). Unlike Gd(III), Lu(III) is not paramagnetic because it has no uncoupled electrons. If coordinated with porphyrins, Lu(III) may produce low state-mixing between the singlet and triplet states of porphyrins. These properties can result in relatively lower phosphorescence intensity and higher fluorescence intensity for Lu-porphyrins than those for Gd-porphyrins, which might lead to comparable phosphorescence and fluorescence emission intensities.[18]

For biomedical applications, the water solubility and cell permeability of a metalloporphyrin, which are strongly dependent on the free porphyrin base, must be considered. Very recently, a novel porphyrin, sinoporphyrin sodium (DVDMS), the dominant active compound isolated from the most commonly used photosensitizer, Photofrin®, was found to have significantly higher photoactivity in preclinical studies than that of Photofrin® itself.[24] DVDMS provides higher brightness and greater singlet-oxygen generation than those of other known photosensitizers, including hematoporphyrin, protoporphyrin IX, and Photofrin®.[25] In addition, DVDMS has greater water solubility, chemical stability, and ability to target tumor cells or diseased tissues owing to its advantageous chemical structure.[26] Owing to these advantages of DVDMS, we developed a new, water-soluble Lu(III)-containing porphyrin, Lu(III)-sinoporphyrin sodium (Lu-DVDMS), and investigated its O_2-sensing properties and photosensitivity to develop a potential multifunctional theranostic agent as both photosensitizer and O_2 indicator.

In this work, the luminescence properties, O_2-sensing capability, and photosensitivity of Lu-DVDMS were studied. The UV-visible (UV-vis) absorption and luminescence characteristics of Lu-DVDMS were investigated. The singlet-oxygen quantum yield (Φ_Δ), fluorescence and phosphorescence quantum yields (Φ_P and Φ_F, respectively), and phosphorescence lifetime (τ_P) of Lu-DVDMS were determined. Finally, the dependence of luminescence including the intensity and lifetime on the O_2 concentration was determined.

Experiment

Materials

Anhydrous gadolinium chloride ($GdCl_3$) and 1,3-diphenylisobenzofuran (DPBF) were purchased from J&K Scientific Ltd. Lutetium chloride hexahydrate ($LuCl_3 \cdot 6H_2O$) was procured from Shanghai Diyang Co., Ltd. DVDMS was provided by Professor Qicheng Fang from the Chinese Academy of Medical Sciences. Hematoporphyrin monomethyl ether (HMME) was obtained from Shanghai Xianhui Pharmaceutical Co., Ltd. Methanol was purchased from Tianjin Fuyu Fine Chemical Co., Ltd. High-purity nitrogen and oxygen (99.99%) were obtained from Harbin Liming Co., Ltd. All the reagents and solvents were used as received without further purification.

Preparation of samples

Lu-DVDMS was synthesized following a method described by Srivastava.[27] Briefly, a mixture of imidazole (6 g), DVDMS (12 mg), and excess $LuCl_3 \cdot 6H_2O$ (80 mg) was added to a 250 mL three-necked bottle under Ar flow for 30 min. Then, the mixture was heated to 200 °C and maintained there with magnetic stirring for 2 h under a flow of argon. Then, it was cooled to room temperature and dissolved in methanol to obtain 10 mL of 1 mM Lu-DVDMS solution. The Lu-DVDMS solution was dialyzed twice for 2 h per cycle using methanol as the solvent. By this process, the Lu-DVDMS was isolated from lower-molecular-weight species like imidazole, Lu^{3+}, and Cl^-. Gd-DVDMS was synthesized by the same method except for the use of Gd^{3+} in place of Lu^{3+}. Gd-DVDMS and Lu-DVDMS were characterized by UV-vis absorption spectroscopy and mass spectroscopy, as described in the ESI.†

Measurements

UV-visible absorption spectra were recorded using a miniature fiber optic spectrometer (Ocean Optics QE65000), equipped with a deuterium lamp. The Φ_Δ of Lu-DVDMS was measured based on a relative method.[5] Details of the measurement are provided in the ESI.† A diode laser with emission centered at 405 nm was used to excite Lu-DVDMS. Photoluminescence spectra were recorded using a miniature fiber optic spectrometer (Ocean Optics USB2000). All the spectra were calibrated using a mercury lamp. To determine the luminescence quantum yield of Lu-DVDMS in air-saturated solutions, Gd-DVDMS was used as the reference, and the sample was excited with a 532 nm solid-state laser (CLO Laser DPGL-500L). Details of the measurement are provided in the ESI.† To determine the photoluminescence lifetime of Lu-DVDMS in

methanol, the decay profile was obtained as described in the ESI.†

The uncertainties in the measurements using Gd- and Lu-DVDMS were compared. Standard errors of multiple measurement values for each O_2 concentration were set as the measurement uncertainty. To ensure high SNRs, phosphorescence signals were tuned to exceed 90% of the full scale of the spectrometer by adjusting the integration time.

To determine the dependence of luminescence on the O_2 concentration, the luminescence spectra and phosphorescence decay curves of Lu-DVDMS (500 μM) in methanol solutions were obtained with different concentrations of dissolved O_2. The methanol solution of Lu-DVDMS (500 μM) was placed in a quartz cuvette (1 × 1 × 4 cm), and the O_2 concentration was adjusted by tuning the flow ratio of O_2 and nitrogen on the surface of the solution. The O_2 concentration was monitored using a Clark electrode. All the other conditions were kept constant and all measurements were performed at room temperature at 1 atm pressure.

Results and discussion

Chemical structure and synthesis of Lu-DVDMS

Fig. 1 shows the chemical structures of DVDMS and Lu-DVDMS, as well as the synthesis scheme for Lu-DVDMS. Structurally, DVDMS contains four sodium carboxylate groups, which impart excellent water solubility.[28] Fig. S2 in the ESI† compares the water solubility of DVDMS with that of a typical porphyrin, HMME. In addition, DVDMS has two porphyrin rings linked by an ether group, which afford higher absorption coefficient than those of typical porphyrins.[28]

Absorption of Lu-DVDMS

Fig. 2 shows the normalized absorption spectra of DVDMS and Lu-DVDMS. The absorption spectrum of DVDMS has four Q bands that appear at 506, 538, 576, and 630 nm, and a Soret band appearing between 350 and 450 nm. The absorption spectrum of Lu-DVDMS also exhibits a Soret band, but it is narrower and red-shifted by 15 nm as compared to that of DVDMS. Because the lanthanide ions are larger than the core

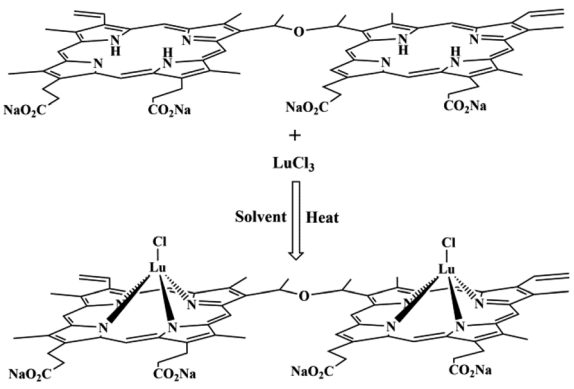

Fig. 1 Synthesis scheme for Lu-DVDMS showing the chemical structures of DVDMS and Lu-DVDMS. Solvent: molten imidazole.

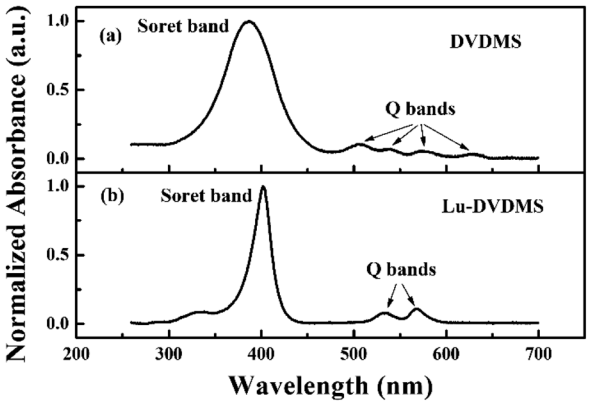

Fig. 2 Normalized absorption spectra of DVDMS and Lu-DVDMS in methanol showing the differences in Q- and Soret bands.

diameter of the porphyrin ligand, the formed lanthanide porphyrin complexes are not planar.[29,30] The red shift mainly originates from the hybrid orbital deformation (HOD) effect due to the distortion in the nonplanar tetrapyrrole macrocycle.[31] The most significant change in the absorption spectrum of Lu-DVDMS is the reduction in the number of Q bands; the absorption spectrum of Lu-DVDMS has only two Q bands (α and β bands[32] at 534 and 568 nm, respectively). The reduction in the number of Q bands agrees well with the Gouterman's four-orbital model, which predicts that, because of the increase in symmetry, the four Q bands of a free porphyrin base will be reduced to two with the formation of a metalloporphyrin.[29] The absorption coefficients (ε) of the three peaks of Lu-DVDMS in methanol were calculated based on the Beer–Lambert law by the analysis of absorption at various Lu-DVDMS concentrations; they are 2.56×10^5 M^{-1} cm^{-1} (402 nm), (3.03×10^4 M^{-1} cm^{-1} (534 nm), and 3.48×10^4 M^{-1} cm^{-1} (568 nm).

Singlet-oxygen quantum yield of Lu-DVDMS

The Φ_Δ of Lu-DVDMS was measured by a relative method[5] using Gd-DVDMS as the reference (0.46 (ref. 33)) and DPBF as the singlet-oxygen-trapping reagent. Details of the measurement are given in Fig. S3 in the ESI.† The calculated Φ_Δ of Lu-DVDMS is 0.23 ± 0.06. The experimental conditions and calculated Φ_Δ of Lu-DVDMS in methanol are listed in Table 1. The Φ_Δ of Lu-DVDMS is lower than those of typical porphyrins[34] such as Photofrin® (0.83 (ref. 35)) but sufficient for use in PDT. The Φ_Δ of a given metalloporphyrin is related to the quantum yield of its triplet state formation.[6] Gd(III) is paramagnetic, and it can

Table 1 Experimental conditions and calculated Φ_Δ of Lu-DVDMS in methanol

Sample	Concentration (μM)	λ_{ex} (nm)	A	k (min^{-1})	Φ_Δ
Gd-DVDMS	2.5	532	0.59	0.083	0.46
Lu-DVDMS	2.5	532	0.58	0.041	0.23

induce a larger extent of mixing between the singlet and triplet states[36] of DVDMS than Lu(III). Thus, Lu-DVDMS has a lower quantum yield of triplet state formation than Gd-DVDMS, and its singlet-oxygen quantum yield is lower than that of Gd-DVDMS.

Luminescence of Lu-DVDMS

Fig. 3(a) shows the normalized luminescence spectrum of Lu-DVDMS obtained with 405 nm laser excitation. The spectrum has peaks at 579, 629, 706, and 776 nm. In general, the first two peaks observed for metalloporphyrins are fluorescence emissions from the singlet states. The lifetime of the last two peaks in the near-infrared region (706, 778 nm) is 167 (±3) μs (shown in Fig. 3(b)); these are considered phosphorescence emissions from the triplet states. Notably, Lu-DVDMS has comparable fluorescence and phosphorescence emission intensities. In addition, Φ_P and Φ_F of Lu-DVDMS in air-saturated methanol were measured by the relative method using Gd-DVDMS as reference (details of the measurement are provided in the ESI, Fig. S4†). The Φ_P and Φ_F of Lu-DVDMS are 0.33 and 0.32%, respectively. Remarkably, the Φ_P of Lu-DVDMS in methanol is two orders of magnitude higher than those of previously reported Lu-porphyrins (*e.g.*, Lu-tetrabenzoporphyrin).[23]

Fig. 3(a) also shows the normalized luminescence spectrum of Gd-DVDMS recorded under the same experimental conditions. The fluorescence emission of Gd-DVDMS is much weaker than its phosphorescence emission.[33] The singlet and triplet states of porphyrins are pure, but the HAE makes these "impure". The mechanism underlying HAE can be explained by spin–orbit coupling (SOC). These states of porphyrins can be perturbed by the nearby nuclear magnetic field of heavy atoms, which mixes pure singlet and triplet states to produce states with a mixed character in spin multiplicity (state mixing).[37] HAE causes intersystem crossing (ISC) from the lowest excited singlet state (S_1) to the lowest triplet state (T_1) and enables the forbidden singlet–triplet transition,[37] *e.g.*, the transition from T_1 to the ground state, *i.e.*, phosphorescence emission. The stronger the heavy atom effect is, the larger the extent of state mixing and the stronger the phosphorescence emission. Paramagnetism has also been reported to mix states.[38–40] The phosphorescence-inducing effect defined in this work is related to both HAE and paramagnetism. As reported by Wang *et al.*,[5] the relatively strong RTP of Gd-porphyrin results from the special energy levels, strong paramagnetism, and HAE of Gd(III). The latter two provide Gd-porphyrins with a large extent of state mixing and thus strong phosphorescence. In contrast, Lu(III) does not exhibit paramagnetism because it has no uncoupled electrons, and thus, it induces less mixing between the singlet and triplet excited states of DVDMS. The relatively weak phosphorescence-inducing effect of Lu(III) suppresses the phosphorescence of Lu-DVDMS ($\Phi_P = 0.33\%$), and thus its RTP is weaker than that of Gd-DVDMS ($\Phi_P = 1.5\%$). This decrease in RTP enables a relatively stronger fluorescence emission of Lu-DVDMS ($\Phi_F = 0.32\%$) than that of Gd-DVDMS ($\Phi_F = 0.13\%$). Note that the phosphorescence-to-fluorescence intensity ratio (I_P/I_F) of Gd-DVDMS is too high (>10) to realize ratiometric O_2 sensing.[33] However, the relatively weak phosphorescence-inducing effect of Lu(III) balances the phosphorescence and fluorescence emissions of DVDMS by energy allocation between the singlet and triplet excited states. This result points to the great potential of Lu-DVDMS in the ratiometric detection of analytes.

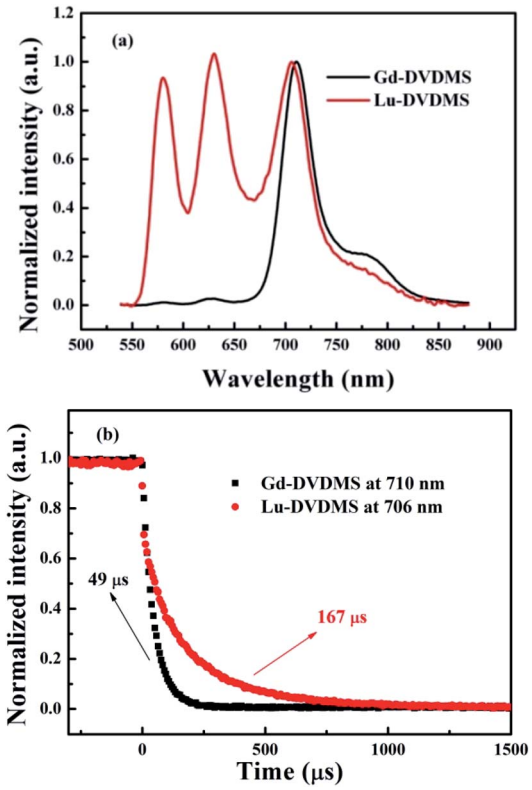

Fig. 3 (a) Normalized luminescence spectra and (b) luminescence decay curves for Gd- and Lu-DVDMS in methanol under excitation with a 405 nm laser.

As shown in Fig. 3(b), Lu-DVDMS has a longer τ_P (167 μs) than that of Gd-DVDMS (49 μs), which also indicates that Lu(III) induces less mixing between the singlet and triplet excited states, and thus leads to weaker phosphorescence emissions and stronger fluorescence emissions. Further, high SNRs for both phosphorescence and fluorescence emissions can be obtained simultaneously for Lu-DVDMS because of its comparable phosphorescence and fluorescence intensities.

Fluctuations of the I_P/I_F for Lu-DVDMS

Fig. 4 shows the fluctuations in the I_P/I_F values of Gd- and Lu-DVDMS in air-saturated solutions in spectra obtained using the same method (using the full scale of the spectrometer by adjusting the integration time). For comparison, the values of the experimentally determined ratios are normalized by their mean values. Clearly, the fluctuations in the I_P/I_F for Lu-DVDMS are much smaller, approximately one-sixth of that for Gd-DVDMS. The lower fluctuation with Lu-DVDMS is due to the simultaneous achievement of high SNRs for both phosphorescence and

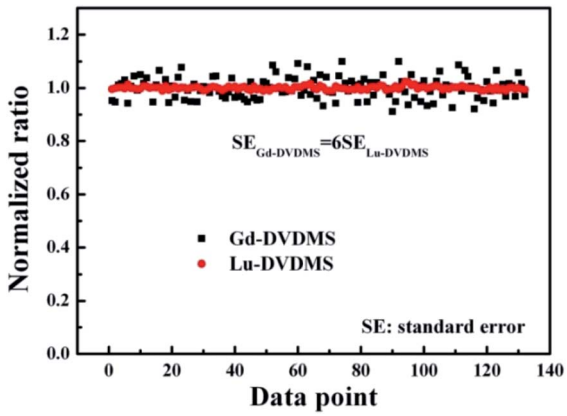

Fig. 4 Fluctuations in I_P/I_F for Gd- and Lu-DVDMS in air-saturated solutions under excitation at 405 nm using the same method. (To ensure high SNRs, phosphorescence signals were tuned to exceed 90% of the full scale of the spectrometer by adjusting the integration time.)

fluorescence emissions. This demonstrates the superiority of Lu-DVDMS over Gd-DVDMS in ratiometric O_2 sensing.

Energy transfer processes in Lu-DVDMS

Fig. 5 shows the energy transfer processes available for Gd- and Lu-DVDMS. The Φ_P of Gd-DVDMS (1.5%) is five times higher than that of Lu-DVDMS (0.33%), while the τ_P of Gd-DVDMS (49 μs) is approximately one-third that of Lu-DVDMS (167 μs). The lower Φ_P and longer τ_P of Lu-DVDMS indicate that the degree of mixing between its singlet and triplet states is lower than that in Gd-DVDMS. This may be due to the stronger paramagnetism of Gd(III). Gd(III) has seven uncoupled electrons in the 4f sub-shell, which induce stronger paramagnetism. Meanwhile, Lu(III) does not have uncoupled electrons and thus, is not paramagnetic, resulting in a lower degree of state mixing;[18] therefore, its Φ_P is lower and τ_P is longer. Thus, the phosphorescence-inducing effect of Lu(III) is lower than that of Gd(III). This also results in a lower Φ_Δ of Lu-DVDMS. Considering the balanced phosphorescence and fluorescence emissions in Lu-DVDMS, it is reasonable to sacrifice the singlet-oxygen generation efficiency. Table 2 compares the photophysical and photochemical properties of Gd- and Lu-DVDMS.

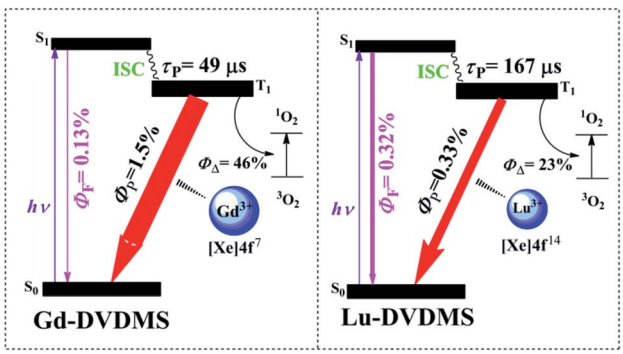

Fig. 5 Energy transfer processes in Gd- and Lu-DVDMS.

The relationship between the phosphorescence quantum yield (Φ_P) and the lifetime (τ_P) can be written as eqn (1),[6]

$$\Phi_P = \Phi_T k_P \tau_P, \quad (1)$$

where Φ_T represents the quantum yield of the triplet state, and k_P is the rate constant of phosphorescence transition. Evidently, the phosphorescence quantum yield is related not only to the lifetime but also to Φ_T and k_P. The paramagnetism of Gd induces a larger HAE and extent of mixing between the singlet and triplet states. In turn, the larger extent of state mixing shortens the triplet lifetime of Gd-DVDMS. Further, it enhances the energy transfer from the singlet state to the triplet state and *vice versa*, which increases the triplet state quantum yield and rate constant of phosphorescence transition for Gd-DVDMS. Thus, although Gd-DVDMS has a shorter lifetime than Lu-DVDMS, it also has a larger triplet state quantum yield and phosphorescence transition rate constant than Lu-DVDMS. This is the reason the phosphorescence of Gd-DVDMS is much stronger than that of Lu-DVDMS, whereas its lifetime is shorter.

Oxygen-sensing properties of Lu-DVDMS

To study the O_2-sensing properties of Lu-DVDMS, luminescence spectra of its solutions with different concentrations of dissolved O_2 were recorded. Fig. 6(a) shows the luminescence spectra of Lu-DVDMS with 0, 160, and 400 μM O_2. Whereas the phosphorescence emission is quenched effectively by O_2, the fluorescence emission remains unchanged. The ratiometric method here is based on the ratio of the phosphorescence intensity (integrated from 704 to 708 nm) over the fluorescence intensity (integrated from 627 to 631 nm) intensity. Based on the ratios for different concentrations of O_2, the Stern–Volmer plot for Lu-DVDMS was obtained (Fig. 6(b)). Good linearity is found in the range of 0 to 400 μM, which can be easily calibrated for application. The calibration curve for Lu-DVDMS is as follows:

$$R_0/R = 0.9840 + 0.0024[O_2] \quad (2)$$

where $[O_2]$ represents the dissolved oxygen concentration.

To study the lifetime response of the Lu-DVDMS phosphorescence *versus* O_2 concentration, the phosphorescence decay curves of Lu-DVDMS in solutions with different concentrations of dissolved O_2 were recorded. Fig. 7(a) shows the decay curves of Lu-DVDMS phosphorescence in solutions with 0, 160, and 400 μM O_2. The lifetime under the degassed condition is 239 μs and decreases with increase in O_2 concentration. Based on the lifetimes with different concentrations of O_2, the lifetime Stern–Volmer plot for Lu-DVDMS was obtained (Fig. 7(b)). Good linearity is also found with this variable in the range of 0 to 400 μM O_2. The calibration curve for Lu-DVDMS is given as follows:

$$\tau_0/\tau = 0.9517 + 0.0034[O_2] \quad (3)$$

Table 2 Comparison of the photophysical and photochemical properties of Gd- and Lu-DVDMS[a]

Sample	Φ_Δ	Φ_F (%)	Φ_P (%)	P/F	τ_P (μs)	Measurement uncertainty for P/F
Gd-DVDMS	0.46	0.13	1.50	>10	49	6*a*
Lu-DVDMS	0.23	0.32	0.33	≈1	167	*a*

[a] a: a relative value; P: phosphorescence; F: fluorescence.

Based on τ_0 and K_{SV}, the oxygen quenching rate constant is calculated to be 14.2 s^{-1}, which is comparable to that of Pd-porphyrin.[19]

The stability of the O_2 indicator is very important for practical applications. Fig. S5(a)† shows the stability of Lu-DVDMS over two months: there is almost no decrease in the phosphorescence emission after storage for 2 months in methanol at room temperature. The storage times for other reported metalloporphyrins are also several months.[41–43] Photostability is another important parameter for all sensing materials, particularly if extended operation is required. Fig. S5(b)† shows the continuous fluorescence (black) and phosphorescence (red) signals of Lu-DVDMS (500 μM) under irradiation with a 405 nm laser at 2 mW cm^{-2} for 120 min. There is no obvious decrease in either the fluorescence or phosphorescence signal of Lu-DVDMS over an extended irradiation time.

To determine the response time of the Lu-DVDMS phosphorescence-to-fluorescence ratio in the sensing of O_2, the change in the ratio upon switching between different O_2 concentrations is shown in Fig. S6.† The ratio increases gradually upon switching from air to nitrogen. Then, it remains unchanged in the nitrogen environment. Thereafter, the phosphorescence intensity drops quickly upon switching from nitrogen to oxygen, with the emission intensity decreasing from its maximum value to a minimum one in 2 min.

On the other hand, based on the intensity Stern–Volmer plot for Lu-DVDMS and the results of Fig. S6,† the precision of O_2 sensing using Lu-DVDMS is better than 0.5 μM in the 0–400 μM oxygen detection range.

Thus, compared with other phosphorescent photosensitizers, Lu-DVDMS can serve as a photosensitizer with ratiometric O_2-sensing ability in PDT.

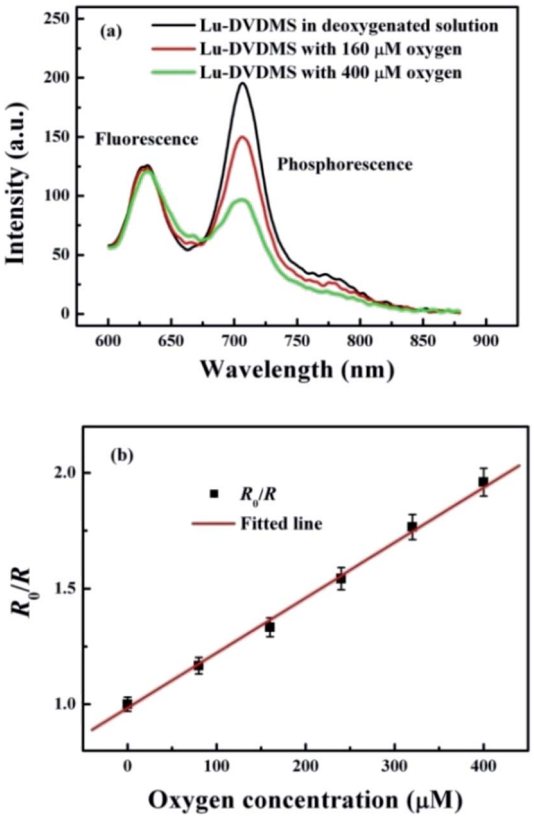

Fig. 6 (a) Luminescence spectra of Lu-DVDMS in solutions with 0, 160, and 400 μM dissolved O_2 under excitation at 405 nm. (b) The intensity Stern–Volmer plot for Lu-DVDMS.

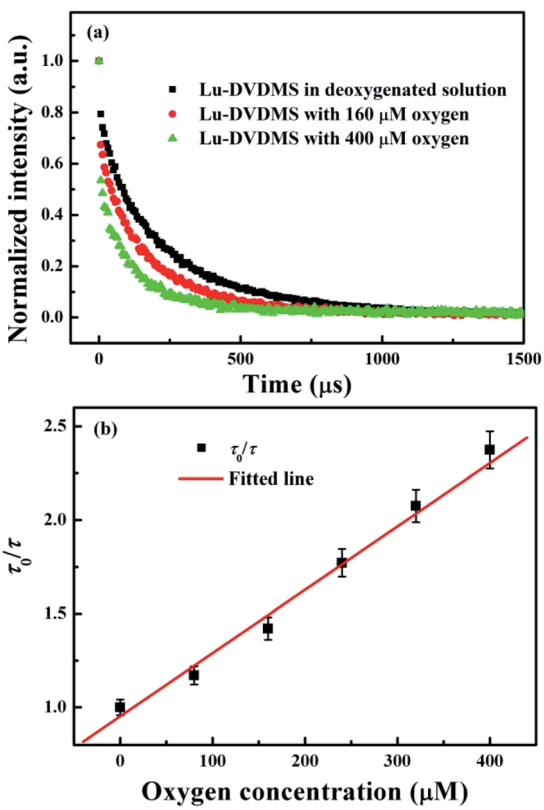

Fig. 7 (a) Phosphorescence decay curves of Lu-DVDMS in solutions with 0, 160, and 400 μM O_2 under excitation at 405 nm. (b) The lifetime Stern–Volmer plot for Lu-DVDMS.

Conclusion

The photosensitivity, luminescence, and O_2-sensing properties of Lu-DVDMS were studied. Lu-DVDMS has high water solubility, stability, and photostability. Lu-DVDMS is also determined to be photosensitive, with $\Phi_\Delta = 0.23 \pm 0.06$, which is sufficient for PDT. The Φ_P and Φ_F of Lu-DVDMS estimated by the relative method are 0.33 and 0.32%, respectively. The I_P/I_F of Lu-DVDMS is ~1, which is suitable for ratiometric O_2 sensing. The relatively weak phosphorescence-inducing effect of Lu(III) leads to the balance between the intensities of phosphorescence and fluorescence emissions because Lu(III) is not paramagnetic unlike paramagnetic Gd(III). The fluctuation of I_P/I_F for Lu-DVDMS is approximately one-sixth of that of I_P/I_F for Gd-DVDMS, which is due to the high SNR achieved for both phosphorescence and fluorescence emissions. The intensity and lifetime Stern–Volmer plots of Lu-DVDMS were found to be linear, $R_0/R = 0.9840 + 0.0024[O_2]$ and $\tau_0/\tau = 0.9517 + 0.0034[O_2]$, respectively. Further, fast response and recovery times (<2 min) in the detection of O_2 were achieved with Lu-DVDMS. The precision for O_2 sensing using Lu-DVDMS is higher than 0.5 μM in the 0–400 μM oxygen detection range. Therefore, Lu-DVDMS is a potential phosphorescent photosensitizer with the capability for ratiometric O_2 sensing.

Conflicts of interest

There are no conflicts to declare.

Acknowledgements

This work was supported in part by the National Natural Science Foundation of China [Grant No. 61905132, 11947222, 61805128, 81741113, and 11747156], the Natural Science Foundation of Shandong Province [Grant No. ZR2017QF002], and the China Postdoctoral Science Foundation [Grant No. 2019M662425 and 2017M622253].

Notes and references

1 Y. Ma, X. Li, A. Li, P. Yang, C. Zhang and B. Tang, *Angew. Chem., Int. Ed.*, 2017, **56**, 13752–13756.
2 Z. Yu, P. Zhou, W. Pan, N. Li and B. Tang, *Nat. Commun.*, 2018, **9**, 5044.
3 W. Zhang, J. Lu, X. Gao, P. Li, W. Zhang, Y. Ma, H. Wang and B. Tang, *Angew. Chem., Int. Ed.*, 2018, **130**, 4985–4990.
4 T. J. Dougherty, C. J. Gomer, B. W. Henderson, G. Jori, D. Kessel, M. Korbelik, J. Moan and Q. Peng, *J. Natl. Cancer Inst.*, 1998, **90**, 889–905.
5 P. Wang, F. Qin, L. Wang, F. Li, Y. Zheng, Y. Song, Z. Zhang and W. Cao, *Opt. Express*, 2014, **22**, 2414.
6 P. Wang, F. Qin, Z. Zhang and W. Cao, *Opt. Express*, 2015, **23**, 22991–23003.
7 C. Li, S. Li, B. Xie, H. Cheng, M. Zhang, X. Zhang, W. Qiu, W. Liu and X. Wang, *Biomaterials*, 2018, **151**, 1–12.
8 L. Chen, L. Lin, Y. Li, H. Lin, Z. Qiu, Y. Gu and B. Li, *J. Lumin.*, 2014, **152**, 98–102.
9 A. D. Shaw, Z. Li, Z. Thomas and C. W. Stevens, *Crit. Care*, 2002, **6**, 76–80.
10 F. B. Bolger and J. P. Lowry, *Sensors*, 2005, **5**, 473–487.
11 W. L. Rumsey, J. M. Vanderkooi and D. F. Wilson, *Science*, 1988, **241**, 1649–1651.
12 D. B. Papkovsky and R. I. Dmitriev, *Chem. Soc. Rev.*, 2013, **42**, 87–8732.
13 G. Zhang, G. M. Palmer, M. W. Dewhirst and C. L. Fraser, *Nat. Mater.*, 2009, **8**, 747–751.
14 H. Hochreiner, I. Sanchezbarragan, J. Costafernandez and A. Sanzmedel, *Talanta*, 2005, **66**, 611–618.
15 M. Valledor, J. C. Campo, F. Ferrero, I. Sánchez-Barragán, J. M. Costa-Fernández and A. Sanz-Medel, *Sens. Actuators, B*, 2009, **139**, 237–244.
16 Y. Feng, J. Cheng, L. Zhou, X. Zhou and H. Xiang, *Analyst*, 2012, **137**, 4885–4901.
17 Y. Liu, H. Guo and J. Zhao, *Chem. Commun.*, 2011, **47**, 11471–11473.
18 L. Zang, H. Zhao, J. Hua, F. Qin, Y. Zheng, Z. Zhang and W. Cao, *Sens. Actuators, B*, 2016, **231**, 539–546.
19 L. Zang, H. Zhao, J. Hua, W. Cao, F. Qin, J. Yao, Y. Tian, Y. Zheng and Z. Zhang, *J. Mater. Chem. C*, 2016, **4**, 9581–9587.
20 H. Zhao, L. Zang, Q. Liu, B. Ma, M. Kou, J. Lv and C. Guo, *J. Lumin.*, 2018, **194**, 29–32.
21 H. Zhao, L. Zang, K. Xu, M. Kou and Z. Zhang, *Spectrochim. Acta, Part A*, 2019, **217**, 310–314.
22 E. G. Ermolina, R. T. Kuznetsova, T. A. Solodova, E. N. Tel'Minov, T. N. Kopylova, G. V. Mayer, N. N. Semenishyn, N. V. Rusakova and Y. V. Korovin, *Dyes Pigm.*, 2013, **97**, 209–214.
23 B. Kalota and M. Tsvirko, *Chem. Phys. Lett.*, 2015, **634**, 188–193.
24 Q. Fang, *Chin. J. New Drugs*, 2014, **23**, 1540–1545.
25 X. Wang, H. Wang, S. Zhang, P. Wang, K. Zhang and Q. Liu, *Int. J. Nanomed.*, 2014, **9**, 3077–3090.
26 J. Hu, X. Wang, K. Zhang, P. Wang, X. Su, Y. Li, Z. Huang and Q. Liu, *Anti-Cancer Drugs*, 2014, **25**, 174–182.
27 T. S. Srivastava, *Bioinorg. Chem.*, 1978, **8**, 61–76.
28 L. Zang, H. Zhao, Q. Fang, M. Fan, T. Chen, Y. Tian, J. Yao, Y. Zheng, Z. Zhang and W. Cao, *J. Porphyrins Phthalocyanines*, 2017, **21**, 59–66.
29 X. Zhu, T. Zhang, S. Zhao, W. Wong and W. Wong, *Eur. J. Inorg. Chem.*, 2011, 3314–3320.
30 T. Lv and W. Sun, *J. Inorg. Organomet. Polym.*, 2013, **23**, 200–205.
31 Z. Zhou, C. Cao, Q. Liu and R. Jiang, *Org. Lett.*, 2010, **12**, 1780–1783.
32 X. Shen, W. Lu, G. Feng, Y. Yao and W. Chen, *J. Mol. Catal. A: Chem.*, 2009, **298**, 17–22.
33 L. Zang, H. Zhao, J. Hua, F. Qin, Y. Zheng, Z. Zhang and W. Cao, *Dyes Pigm.*, 2017, **142**, 465–471.
34 A. S. Stasheuski, V. A. Galievsky, V. N. Knyukshto, R. K. Ghazaryan, A. G. Gyulkhandanyan, G. V. Gyulkhandanyan and B. M. Dzhagarov, *J. Appl. Spectrosc.*, 2014, **80**, 813–823.

35 J. Y. Nagata, N. Hioka, E. Kimura, V. R. Batistela, R. S. S. Terada, A. X. Graciano, M. L. Baesso and M. F. Hayacibara, *Photodiagn. Photodyn. Ther.*, 2012, **9**, 122–131.
36 H. Huang and Y. Bu, *J. Phys. Chem. C*, 2019, **123**, 28327–28335.
37 A. S. Carretero, A. S. Castillo and A. F. Gutiérrez, *Crit. Rev. Anal. Chem.*, 2005, **35**, 3–14.
38 A. Arriman, *J. Chem. Soc., Faraday Trans. 2*, 1981, **77**, 1281–1291.
39 H. Huang and Y. Bu, *J. Phys. Chem. C*, 2019, **123**, 28327–28335.
40 B. Minaev, *Spectrochim. Acta, Part A*, 2004, **60**, 3213–3224.
41 A. Fercher, S. M. Borisov, A. V. Zhdanov, I. Klimant and D. B. Papkovsky, *ACS Nano*, 2011, **5**, 5499–5508.
42 X. Wang, J. A. Stolwijk, T. Lang, M. Sperber, R. J. Meier, J. Wegener and O. S. Wolfbeis, *J. Am. Chem. Soc.*, 2012, **134**, 17011–17014.
43 S. Kochmann, C. Baleizão, M. N. Berberan-Santos and O. S. Wolfbeis, *Anal. Chem.*, 2013, **85**, 1300–1304.